Scleral Proteome in Noninfectious Scleritis Unravels Upregulation of Filaggrin-2 and Signs of Neovascularization

Daphne P. C. Vergouwen,[1,2] Josianne C. Ten Berge,[1] Coskun Guzel,[3] Thierry P. P. van den Bosch,[4] Robert M. Verdijk,[4] Aniki Rothova,[1] Theo M. Luider,[3] and Marco W. J. Schreurs[2]

[1]Department of Ophthalmology, Erasmus MC, University Medical Center Rotterdam, Rotterdam, The Netherlands
[2]Department of Immunology, Laboratory Medical Immunology, Erasmus MC, University Medical Center Rotterdam, Rotterdam, The Netherlands
[3]Department of Neurology, Erasmus MC, University Medical Center Rotterdam, Rotterdam, The Netherlands
[4]Department of Pathology, Section Ophthalmic Pathology, Erasmus MC, University Medical Center Rotterdam, Rotterdam, The Netherlands

Correspondence: Daphne P.C. Vergouwen, Department of Ophthalmology, Erasmus University Medical Center, Dr. Molewaterplein 40, 3015GD Rotterdam, The Netherlands; d.vergouwen@erasmusmc.nl.

Received: January 2, 2023
Accepted: March 3, 2023
Published: March 17, 2023

Citation: Vergouwen DPC, Ten Berge JC, Guzel C, et al. Scleral proteome in noninfectious scleritis unravels upregulation of filaggrin-2 and signs of neovascularization. *Invest Ophthalmol Vis Sci.* 2023;64(3):27. https://doi.org/10.1167/iovs.64.3.27

Purpose. Scleritis is a severe inflammatory ocular disorder with unknown pathogenesis. We investigated healthy sclera as well as sclera affected by noninfectious scleritis for differentially expressed proteins using a mass spectrometry approach.

Methods. We collected scleral samples of enucleated eyes due to severe noninfectious scleritis ($n = 3$), and control scleral tissues ($n = 5$), all exenterated eyes for eyelid carcinomas ($n = 4$), or choroidal melanoma ($n = 1$) without scleral invasion. Samples were prepared for the nano liquid-chromatography mass spectrometer (LC-MS), data were analyzed using proteomics software (Scaffold), and is available via ProteomeXchange (identifier PXD038727). Samples were also stained for immuno-histopathological evaluation.

Results. Masspc spectrometry identified 629 proteins within the healthy and diseased scleral tissues, whereof collagen type XII, VI, and I were the most abundantly expressed protein. Collagen type II-XII was also present. Filaggrin-2, a protein that plays a crucial role in epidermal barrier function, was found upregulated in all scleritis cases. In addition, other epithelial associated proteins were upregulated (such as keratin 33b, 34, and 85, epiplakin, transglutaminase-3, galectin 7, and caspase-14) in scleritis. Further, upregulated proteins involved in regulation of the cytoskeleton (vinculin and myosin 9), and housekeeping proteins were found (elongation factor-2 and cytoplasmic dynein 1) in our study. Upregulation of filaggrin-2 and myosin-9 was confirmed with immunohistochemistry, the latter protein showing co-localization with the endothelial cell marker ETC-related gene (*ERG*), indicating neovascularization in scleral tissue affected by scleritis.

Conclusions. We found upregulation of filaggrin-2 and signs of neovascularization in scleral tissue of patients with noninfectious scleritis. Further research, ideally including more scleritis cases, is needed to validate our findings.

Keywords: scleritis, pathogenesis, mass spectrometry, proteomics, histopathology, filaggrin-2

Scleritis is a severe inflammation of the sclera, the outer protecting wall of the eye. It is characterized by intense pain and potentially destructive complications, such as visual loss and globe perforation. It usually affects the middle-aged population, having a high impact on the quality of life.[1–3]

The pathophysiology of noninfectious scleritis is poorly understood, however, a crucial role for the immune system in scleritis is accepted. Around half of affected patients have associated systemic immune mediated diseases, such as rheumatoid arthritis (RA), or granulomatosis with polyangiitis (GPA). Various hypotheses on immunopathology have been proposed, including both cell-mediated and humoral antibody mediated mechanisms. Histopathological studies of scarcely available material revealed two types of immune mediated scleritis.[4] In the first necrotic areas where polymorpho-nuclear granulocytes and macrophages were seen, they were predominantly surrounded by B-lymphocytes, and the other consisting of a nonspecific chronic leukocyte infiltration, mainly T-lymphocytes, without necrosis.[5–7] In addition, extracellular matrix components are suspect to be affected in the initial phase of scleritis.[8,9]

The exact cells and molecular substances involved in the pathogenesis of scleritis remain to be elucidated. Recently,

the scleral proteome was characterized using mass spectrometry, a highly innovative and powerful technique.[10,11] Because this technique has the potential to advance knowledge into the pathophysiology of scleritis, we performed a comparative proteomic analysis of sclera affected by noninfectious scleritis versus healthy sclera, using mass spectrometry.

Methods

Subjects and Sample Collection

We included three enucleated human donor eyes affected by noninfectious scleritis, which had undergone routine histopathological investigation at the Erasmus MC, Rotterdam. Indications for enucleation were extreme and uncontrollable pain due to scleritis, or globe perforation. One of these eyes was enucleated directly post-mortem for diagnostic and research purposes, in agreement with the patient and family wishes. In addition, five human donor eyes following exenteration for eyelid carcinoma (squamous cell carcinoma or basal cell carcinoma; $n = 4$), or choroidal melanoma ($n = 1$) without any scleral involvement, were included as control samples/tissues. Clinical data were collected retrospectively from medical files, and included age at onset, gender, scleritis subtype and location, time interval between the onset of scleritis and enucleation, complications of scleritis, etiology, and systemic and local immunosuppressive treatment at the moment of enucleation. This study was conducted according to the Declaration of Helsinki, and approved by the medical ethical committee (Erasmus MC, Rotterdam), under study number NL71698.078.19.

Sample Preparation

The methodological procedure is shown in Figure 1. Freshly enucleated eyes were fixated in neutral buffered formalin 10% after evaluation, following a normal diagnostic procedure. After processing, the formalin-fixed paraffin embedded (FFPE) block was cut at 4 µm sections using a microtome, and mounted on glass slides. Slides were stored at room temperature (RT) until further processing. For mass spectrometry, scleral tissue was carefully scraped off the glass slides using a scalpel and binocular preparation microscope, without encountering episcleral, conjunctival, or choroidal tissue. For normalization purposes, a similar surface area (±1500 µm × 370 µm × 4 µm) was scraped of all samples. Scleral tissue was placed in an Eppendorf tube for enzymatic digestion to perform mass spectrometry (see Fig. 1).

Histopathology

For diseased samples, standard haematoxylin and eosin staining was performed with routine staining protocols using an automated staining system (HE600; Ventana Medical Systems, Tucsen, AZ, USA). Immunohistochemistry was performed with an automated, validated, and accredited staining system (Ventana Benchmark ULTRA; Ventana Medical Systems) using an ultraview universal DAB detection kit. In brief, following deparaffinization and heat-induced antigen retrieval, the tissue samples were incubated according to their optimized time with the antibody of interest. Incubation was followed by hematoxylin II counter stain for 8 minutes and then a blue coloring reagent for 8 minutes according to the manufacturer's instructions (Ventana Medical Systems). Routine immunohistochemical testing for inflammatory cell infiltrate was performed using antibodies to CD3 (Clone: 2GV6, #790-4341; Ventana Medical Systems), CD4 (Clone: SP35, #790-4423; Ventana Medical Systems), CD8 (Clone: C8/144B, #M7103; DAKO), CD68 (Clone: KP-1, #790-2931; Ventana Medical Systems), CD163 (Clone: MRQ-26, #760-4437; Cell Marque), and HLA-DR (Clone: CR3/43; #M0775, DAKO). Two proteins were selected because of their highest significance in the initial analysis, these proteins were immunohistochemically stained for validation purposes, that is, anti-filaggrin-2 (Clone: polyclonal, #HPA028699; Sigma Aldrich) and anti-myosin-9 (Clone: polyclonal, #HPA001644; Sigma Aldrich). Thereby, double staining procedures with anti-CD163 (Clone: MRQ-26, #760-4437; Cell Marque), and anti-ETS-related gene (anti-ERG), a transcription factor expressed in vascular endothelial cells (Clone: EPR3864, #790-4576; Ventana Medical Systems), were performed to further characterize the involved cell population.

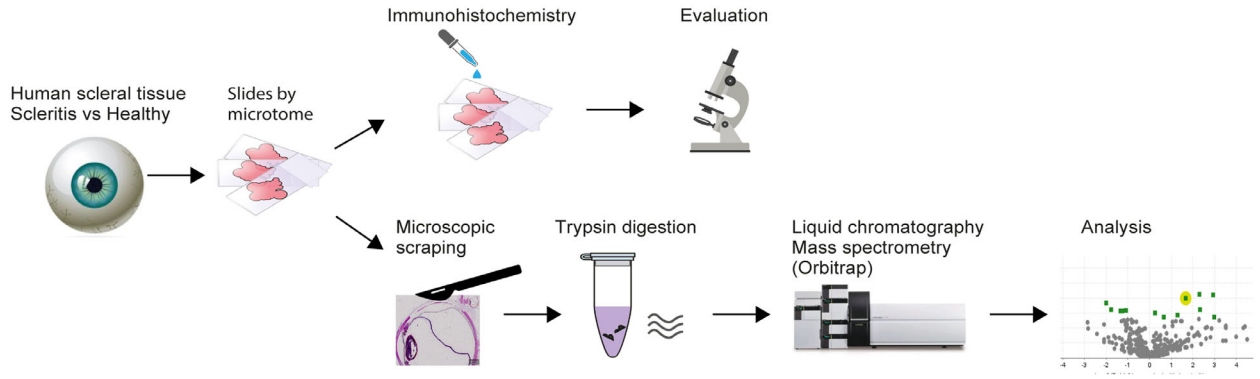

Figure 1. Processing of scleral tissue samples for histopathological and mass spectrometry analysis. Fresh enucleated eyes from human donors (3 affected by scleritis, and 5 due to eyelid carcinoma without any scleral involvement) were fixated in neutral buffered-formalin 10%. The formalin fixed paraffin embedded (FFPE) block was cut at 4 µm sections using a microtome, and mounted on slides. Slides were used for immunohistochemistry or for mass spectrometry, scleral tissue was carefully scraped off slides using a scalpel and binocular preparation microscope, without encountering episcleral, conjunctival, or choroidal tissue. Scleral tissue was placed in an Eppendorf tube for enzymatic digestion, where after mass spectrometry was performed.

Investigative Ophthalmology & Visual Science

Tissue Digestion and Mass Spectrometry

All scleral tissues were deparaffinized using xylene and a descending alcohol series, and finally were placed in 300 mM Tris buffer pH8. A volume of 200 ul 0.1% Rapigest (Waters, Milford, MA, VS) diluted in 50 mM ammonium bicarbonate was added to the samples, and sonified for 1 minute at 85% amplitude. Hereafter, samples were heated for 5 minutes at 99°C. After addition of 2 µL 500 mM dithiothreitol (Sigma-Aldrich), samples were incubated for 30 minutes at 60°C. To the samples, 6 µL 500 mM iodoacetamide (Sigma-Aldrich) was added and incubated for 30 minutes at RT in the dark, and 4 uL 500 mM DTT to quench the alkylation reaction before trypsin addition. A volume of 20 µL (0.1 µg trypsin/µL tris buffer; Promega, Product no: V5280) was added and the samples were digested for 16 hours at 37°C on a Thermomixer with shaking at 400 rpm. To stop the reaction 5 uL, 50% Trifluoroacetic acid (TFA) was added to reach pH <2.0 and incubated for 30 minutes at 37°C on a Thermomixer with shaking at 400 rpm. Digested samples were centrifuged at 14,000 rpm for 10 minutes, and, subsequently, the supernatant was transferred to a new Eppendorf tube. Before loading on the nano LC-MS, the sample was diluted 20 times. The LC-MS acquisition was conducted on a nano-LC system (Ultime 3000 RSLC; Thermo Fisher Scientific, Germering, Germany) coupled to a field asymmetric ion mobility spectrometry (FAIMS) tribrid mass spectrometer (Thermo Fisher Scientific, San Jose, CA, USA) using a 90 minutes gradient 4% to 28% ACN and 4 consecutive FAIMS CV fractions of −40, −50, −75, and −90 volts. Instrumental settings and further parameters used were described recently with minor adaptations. In short, peptides were separated on a 25 cm analytical nano-LC column using a 90-min gradient (from 4% to 24% in solvent B, i.e., 80% acetonitrile and 0.08% formic acid). Electrospray ionization was used with coated silica nano electrospray emitters (spray voltage of 2.2 kV). A data-dependent acquisition MS method was used to identify proteins in scleritis tissue, with precursor masses excluded after fragmentation for 60 seconds. The Orbitrap survey scan ranged from 375 to 1500 m/z with a resolution of 120,000 and AGC target of 400,000. FAIMS source was used to collect ion mobility fractions at different compensation voltages (i.e. −40, −55, −70, and −85V).[12] UV-traces of diseased samples and controls were comparable.

Bioinformatics

Proteins were identified using the Uniprot/Swissprot database (version 2012_012, human taxonomy, 20,395 entries) using the MASCOT search engine with a one-peptide-minimum, a protein threshold of 99%, and a peptide threshold of 95% using the Mascot search engine. The data were directly searched against a decoy database. Analyses were performed using the Scaffold software for proteomics, and spectral counts were used as a semiquantitative measure (Proteome Software). An independent sample *t*-test on normalized total spectral counts was used to identify differentially expressed proteins, considering multiple testing correction using the Benjamini-Hochberg method.[13] The mass spectrometry proteomics data have been deposited to the ProteomeXchange Consortium via the PRIDE[14] partner repository with the dataset identifier PXD038727 and 10.6019/PXD038727.

Results

Cases

Baseline characteristics of three scleritis tissues and controls are shown in Table 1. The first tissue was derived from a female patient with RA, and was affected by a diffuse panscleritis leading to visual impairment. The second tissue was derived from a female patient with RA as well, and was affected by a posterior scleritis. The third tissue originated from a male patient, and was affected by anterior necrotizing scleritis, which resulted in globe perforation. At the time of enucleation, scleritis was active in all cases.

Histopathological Findings

Figure 2 shows the histopathological findings of affected scleral tissues compared to healthy scleral tissue. Scleral edema within the collagen fibrils was seen in all tissues affected by scleritis, whereas necrosis was observed only in the third case. CD4 and CD8 staining for, respectively, helper T-cells and cytotoxic T-cells showed these to be the main inflammatory cell components in cases 1 and 2. Staining with CD68, CD163, and HLA-DR, a marker for major histocompatibility complex (MHC) class II expression, identified activated macrophages in all cases. CD20 staining for B-cells showed minimal positivity in cases 1 and 2, and was negative in case 3.

Differentially Expressed Proteins

A total number of 629 proteins in 519 protein clusters were identified by mass spectrometry in healthy and diseased scleral tissues. A list of the 10 most abundantly present proteins is shown in Table 2, whereas the complete database can be visited at the online PRIDE repository. Collagen type XII, VI, and I were the most abundantly present protein, other collagen types present in scleral tissue are II-XI, XIV-XVI, XVIII, XIX, XXII, XXIII, XXV, and XXVI. The comparative proteomic analysis between scleritis and healthy is shown in Figure 3, wherein the Venn diagram shows that 146 proteins are exclusively found in scleral tissues affected by scleritis. Solely filaggrin-2 was found to be significantly upregulated in scleritis (see Fig. 3B). The heatmap of protein expression in diseased scleral tissue compared to control sclera shows the most prominent differentially expressed proteins (see Fig. 3C). Filaggrin-2 was found to be clearly upregulated in all scleritis cases, whereas low in healthy scleral tissue. Additional post-translational modification analysis revealed that filaggrin-2 was citrullinated in 1 out of 3 scleritis cases. Among other differentially expressed proteins with highest fold-change, were the epithelial associated proteins keratin 33b, 34, and 85, epiplakin, transglutaminase-3, galectin 7, and caspase-14. In addition, we found proteins involved in regulation of the cytoskeleton (vinculin and myosin-9), and housekeeping proteins (elongation factor-2 and cytoplasmic dynein 1) to be elevated in scleritis (see Fig. 3; Supplementary Table S1).

Validation by Immunohistochemistry

Filaggrin-2 immunohistochemistry showed staining of extracellular matrix of the scleral stroma in scleritis compared

Investigative Ophthalmology & Visual Science

Table 1. Baseline Characteristics of Scleral Tissues Affected by Scleritis ($N = 3$) and Control Scleral Tissues ($N = 5$)

Tissue No	Gender	Age*	Laterality	Scleritis Subtype	Etiology	Complication Scleritis	Onset Scleritis to Enucleation (Months)	Systemic Treatment†	Local Treatment†	Eye
1	F	47	Bilateral	Diffuse panscleritis	SD	VI	30	Prednisone 20 mg a day and CYC	No	OD
2‡	F	47	Bilateral	Posterior	SD	VI	21	Dexamethasone 2 mg a day	No	OS
3	M	73	Unilateral	Anterior necrotizing	Idiopathic	Globe perforation	1	No	No	OS
4	M	61	–	–	–	–	–	–	–	OD
5	M	73	–	–	–	–	–	–	–	OD
6	F	76	–	–	–	–	–	–	–	OD
7	F	61	–	–	–	–	–	–	–	OD
8	M	55	–	–	–	–	–	–	–	OD

SD, systemic disease; VI, visual impairment; CYC, cyclophosphamide.
* At onset scleritis, in patients with scleritis, at enucleation in controls.
† At time of enucleation.
‡ Post-mortem eye.

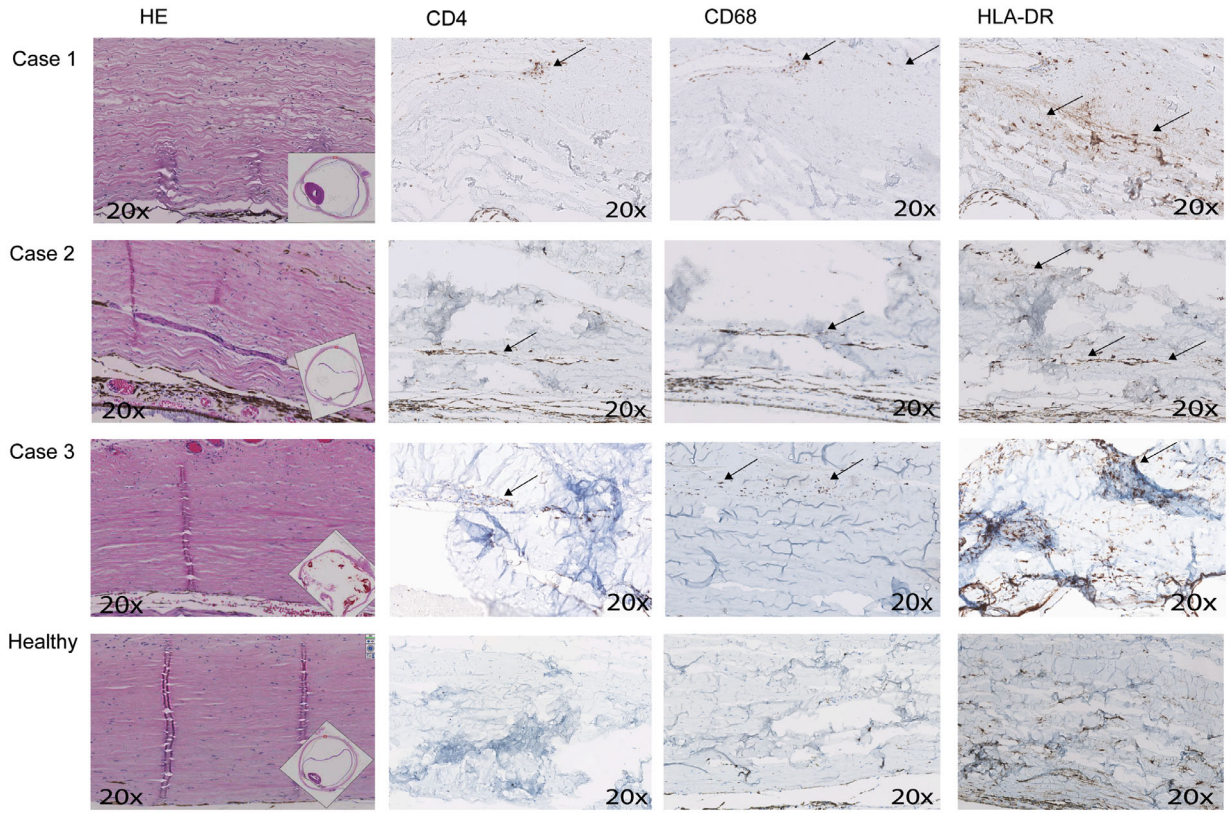

Figure 2. Histopathological findings of scleral tissues affected by scleritis ($N = 3$) versus healthy scleral tissue ($N = 1$). HE staining shows scleral edema within the collagen fibrils in all tissues affected by scleritis, whereas necrosis was seen only in the third case. CD4 staining for helper-T-cells was positive mainly in cases 1 and 2. CD8 staining for cytotoxic T-cells showed a similar staining pattern (figures not shown). Macrophage staining with CD68 and CD163 (figures not shown), and HLA-DR, a marker for major histocompatibility complex (MHC) class II expression, were positive in all cases. CD20 staining for B-cells showed minimal positivity in cases 1 and 2, and was negative in case 3 (figures not shown). All healthy controls show comparable staining patters (only one is shown), with low amounts of CD4, and CD20 positive T-cells and B-cells. A number of resting macrophages and antigen-presenting cells in healthy scleral tissue is seen with moderate CD68, CD163 (figure not shown), and HLA-DR staining. HE, hematoxylin and eosin. Magnification = 20 times.

to absence of staining in controls, which validates the mass spectrometry results (Fig. 4). Further, myosin-9, which stained endothelial and stromal cells, was clearly upregulated in scleritis, confirming the mass spectrometry results. The upregulated myosin-9 positive cell population was further characterized using double staining procedures. No co-localization was found for the macrophage marker CD163. However, immunohistochemistry revealed *ERG* positivity, typical for (progenitor) endothelial cells (see Fig. 4).

Investigative Ophthalmology & Visual Science

Table 2. Top 10 Most Abundantly Present Proteins Identified in Human Scleral Tissue Using Mass Spectrometry ($N = 8$)

UniProt ID	Protein Name	Molecular Weight	Proteinc Function
P02768	Albumin	69 kDa	Regulation of the colloidal osmotic pressure of blood
Q99715	Collagen alpha-1 (XII) chain	333 kDa	Interacts with type I collagen-containing fibrils, extracellular matrix structural constituent conferring tensile strength
P13645	Cluster of keratin, type I cytoskeletal 10	59 kDa	Structural constituent of skin epidermis and plays a role in *S. Aureus* nasal colonization
P35908	Cluster of keratin, type II cytoskeletal 2 epidermal	65 kDa	Role in the establishment of the epidermal barrier on plantar skin
P12111	Collagen alpha-3 (VI) chain	344 kDa	Extracellular matrix structural constituent conferring tensile strength and serine-type endopeptidase inhibitor activity
P04264	Keratin, type II cytoskeletal 1	66 kDa	Structural constituent of skin epidermis. May regulate the activity of kinases via binding to integrin beta-1 (ITB1) and the receptor of activated protein C kinase 1 (RACK1)
P02533	Cluster of keratin, type I cytoskeletal 14	52 kDa	Structural constituent of cytoskeleton and role in keratin filament binding
P35527	Keratin, type I cytoskeletal 9	62 kDa	Keratin filament assembly, important function either in palmar and plantar skin tissue
P02452	Collagen alpha-1(I) chain	139 kDa	Fibril forming collagen, extracellular matrix structural constituent conferring tensile strength
P08670	Cluster of vimentin	54 kDa	Class III intermediate filaments, involved in the stabilization of type I collagen mRNAs for CO1A1 and CO1A2

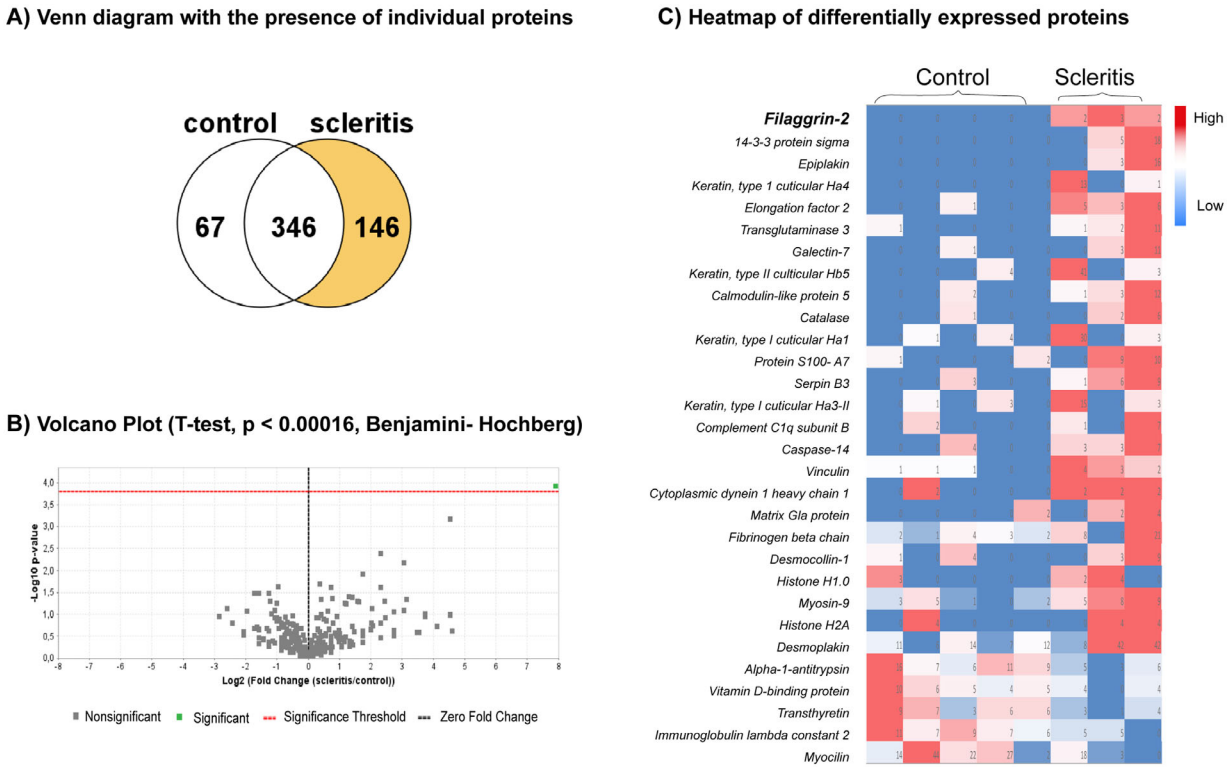

Figure 3. Comparative proteomics of scleral tissue affected by scleritis ($N = 3$) versus control scleral tissue ($N = 5$). (**A**) Venn diagram of the presence of individual proteins in control scleral tissues ($N = 5$) versus scleral tissues affected by scleritis ($N = 3$) analyzed by mass-spectrometry. One hundred forty-six (146) proteins were exclusively found in scleral tissues affected by scleritis. (**B**) Volcano plot of protein differences in scleral tissues affected by scleritis versus control scleral tissues. Only filaggrin-2 was found to be significantly different taking into account the Benjamini-Hochberg method for multiple testing. (**C**) Heatmap of differentially expressed proteins ($N = 30$) in sclera affected by scleritis ($N = 3$) versus control sclera ($N = 5$).

Discussion

Our in-depth proteomic analysis of scleral tissue indicates several interesting proteins, which were significantly upregulated in noninfectious scleritis versus control scleral tissues. Insight in the dysregulated protein pathways in scleritis can help to understand the pathogenesis of this severe ocular disorder.[15] To the best of our knowledge,

Investigative Ophthalmology & Visual Science

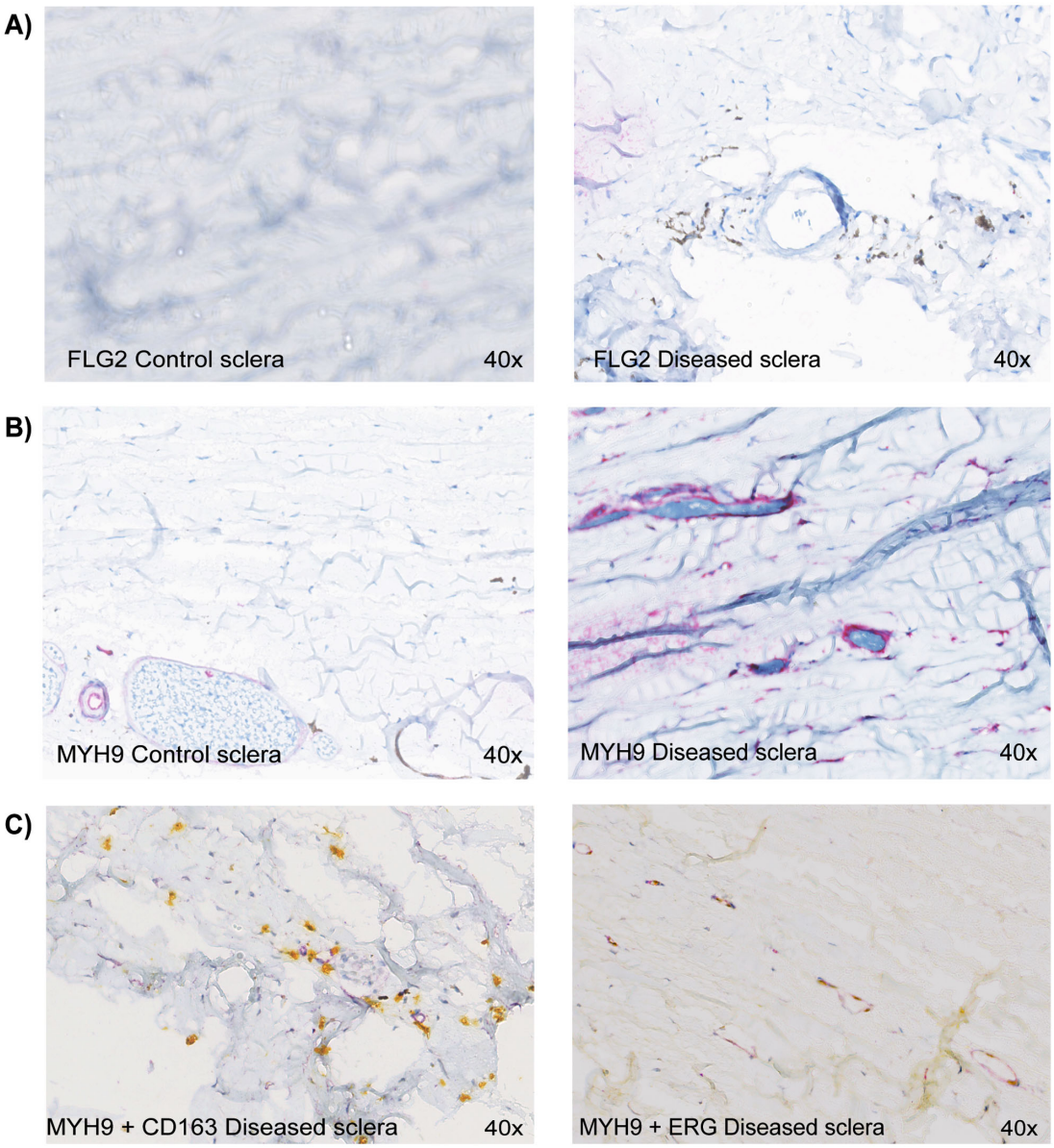

Figure 4. Immunohistochemical validation of filaggrin-2 and myosin-9 upregulation in scleritis, and characterization of myosin-9 positive scleral cells using CD163 and ETS-related gene (*ERG*) transcription factor. (**A**) Filaggrin-2 (FLG2) staining (*brown*) shows extracellular matrix coloring in diseased scleral tissue versus no staining in control scleral tissue. (**B**) Myosin-9 (MYH9) staining (*purple*) is upregulated in the diseased sclera (vascular wall and stromal cells). (**C**) Double staining of diseased sclera with myosin-9 (*purple*) and CD163 (*yellow*, cytoplasmic stain), a macrophage marker, shows little overlap. Double staining with myosin-9 (*purple*) and ETC-related gene (*ERG*) transcription factor, expressed in endothelial cells (*yellow*, nuclear stain), shows extensive overlap. FLG2, Filaggrin-2; MYH9, Myosin-9. Magnification = 40 times.

this is the first report of a tissue proteomic analysis of scleritis.

A previous study into the proteome of healthy scleral tissue proposed the following proteins as possible factors involved in inflammation: S100 proteins, complement factors, cystatin C, vascular cell adhesion molecule-1, and CXC4.[10] Protein S100-A7 was indeed upregulated in our scleritis cases with a fold change of 11. This protein is also called "psoriasin" because it is overexpressed by psoriatic keratinocytes, and it is thought to be a systemic pro-inflammatory mediator in psoriasis. The complement factor C1q subunit B was found to be 7-fold higher in scleritis tissue compared to control tissue in our analysis, reflecting activation of the classical complement system. Other proteins mentioned in these two previous studies were not reproduced in our series.

Filaggrin-2 showed clear upregulation in scleritis and is a relatively recently discovered member of the S100 fused-type proteins. It is essential for cell-cell adhesion to maintain the epidermal barrier, similarly to filaggrin.[16,17] Although we find upregulation of this protein in sclera affected by scleritis, downregulation of this protein is linked to skin diseases, such as atopic dermatitis and psoriasis, and seems to be under control of specific interleukins.[18,19] In anti-filaggrin antibodies, as well as anti-citrullinated filaggrin antibodies, were found to have a pathogenic role.[20,21] In our series, only one scleritis case citrullination of filaggrin-2 could be observed. To the best of our knowledge, filaggrin-2

Investigative Ophthalmology & Visual Science

upregulation was not described previously in scleritis, or other systemic inflammatory disease. The potential role of filaggrin-2 in scleritis is intriguing and requires further investigation.

Several epithelial associated proteins were found within differentially expressed proteins in our study. Epiplakin, keratin 34 (keratin, type I cuticular Ha4), transglutaminase 3 (protein-glutamine gamma-glutamyltransferase), galectin-7, keratin 85 (keratin, type II cuticular Hb5), calmodulin-like protein 5, keratin 33b (keratin, type I cuticular Ha3-II), caspase-14, desmocollin-1, and desmoplakin were found to be upregulated. Epiplakin and transglutaminase 3 are both proteins involved in keratinization.[22,23] Caspase-14 is of importance in cornification via regulation of the filaggrin catabolism, and was found to be upregulated in synovial fluid of patients with RA.[24,25] Whether and how these epithelial associated proteins are involved in the pathogenesis of scleritis is yet unclear. Although proteomic studies show that healthy human eye tissues (conjunctiva, cornea, iris, lens, retina, and choroid/retinal pigment epithelium) contain keratins in low amounts, scleral stroma is not covered by an epithelial layer.[26,27] Upregulation of these markers in the scleral stroma therefore means that they are newly produced. Hypothetically, in an inflammatory milieu, driven by pro-inflammatory cytokines, fibroblasts could change to a pro-fibrotic active phenotype, in which they are called myofibroblasts. Myofibroblasts could produce epithelial associated proteins, and exaggerate the pathological inflammatory process.[28]

Further, several proteins present in scleritis tissues, are known to be involved in (immune) cell activation or regulation via the cytoskeleton (vinculin, myosin-9, and myocilin). Vinculin, a regulating protein of the cytoskeleton, has a role in neutrophil adhesion and spreading, and is known from the anti-citrullinated vinculin antibodies identified in RA.[29–31] Myosin-9 is a cellular protein required for T-cell stimulation within $CD163^{+}$ macrophages, and T-cell mediated killing.[32,33] Using immunohistochemistry, we show that myosin-9 upregulation is predominantly found in cells staining positive for the endothelial cell marker ERG. Because not all these positively stained cells formed a vascular wall structure, we hypothesize that neovascularization takes place in this inflamed tissue under influence of pro-antiogenic factors. In a newly proposed mouse model of scleritis, also signs of angiolymphogenesis were found.[34] In RA, as well as other systemic autoimmune diseases, neovascularization has a clear pathogenic role.[35]

Last, a number of proteins that were found to be upregulated in scleritis in our study, for example, elongation factor-2, cytoplasmic dynein 1, and histones may belong to the housekeeping proteins.[36–38] We believe these proteins are markers for increased cell metabolism and proliferation, being common findings in inflamed tissues. Biomarkers that were previously found to be up- or downregulated in serum or tear fluid in scleritis, including TNF alpha, matrix metalloproteinases, tissue inhibitor of matrix metalloproteinase, or interleukins (IL-1b and IL-22) were not found in our analysis.[39–44]

Our study is limited by the small number of available samples. Tissue biopsies in scleritis are generally contraindicated, as any kind of surgery on scleral tissue may aggravate scleritis. To validate our findings and strengthen conclusions more samples, requiring (inter)national collaborations, should be gathered. Other "omics" approaches could be used to validate findings as well. In addition, in this mass spectrometry based proteomic analysis, we identified the most abundantly present proteins. It is possible that within proteins that are scarcely present in sclera, relevant differences between healthy and diseased sclera could be overlooked. Further, we have not included other inflamed ocular tissue as disease control for comparison with scleritis in this study. Therefore, we cannot exclude that some upregulated proteins found in our study are associated with inflammation in general, and are not specific for scleritis.

In conclusion, we found upregulated proteins in scleritis tissues compared to control scleral tissue a proteomic approach, for example filaggrin-2. Our results open new avenues for clarification of the pathogenesis of noninfectious scleritis, and should stimulate and enable further studies into this severe ocular disease. Future studies may elucidate which proteins serve as biomarkers in the diagnosis and management of scleritis or even identify those which could be therapeutically targeted.

Acknowledgments

The authors wish to thank the pathologist and ophthalmologist of the Albert Schweitzer hospital (Dordrecht, The Netherlands) for kindly providing scleral rest material.

Supported by the Lijf en Leven foundation, this funding organization had no role in the design or conduct of this research.

Disclosure: **D.P.C. Vergouwen**, None; **J.C. Ten Berge**, None; **C. Guzel**, None; **T.P.P. van den Bosch**, None; **R.M. Verdijk**, None; **A. Rothova**, None; **T.M. Luider**, None; **M.W.J. Schreurs**, None

References

1. Watson PG, Hayreh SS, Awdry PN. Episcleritis and scleritis. I. *Br J Ophthalmol*. 1968;52:278–279.
2. Wakefield D, Di Girolamo N, Thurau S, Wildner G, McCluskey P. Scleritis: Immunopathogenesis and molecular basis for therapy. *Prog Retinal Eye Res*. 2013;35:44–62.
3. Sharma SM, Damato E, Hinchcliffe AE, et al. Long-term efficacy and tolerability of TNFalpha inhibitors in the treatment of non-infectious ocular inflammation: An 8-year prospective surveillance study. *Br J Ophthalmol*. 2021;105(9):1256–1262.
4. Hankins M, Margo CE. Histopathological evaluation of scleritis review. *J Clin Pathol*. 2019;72:386–390.
5. Rao NA, Marak GE, Hidayat AA. Necrotizing scleritis. A clinico-pathologic study of 41 cases. *Ophthalmology*. 1985;92:1542–1549.
6. Riono WP, Hidayat AA, Rao NA. Scleritis: A clinicopathologic study of 55 cases. *Ophthalmology*. 1999;106:1328–1333.
7. Usui Y, Parikh J, Goto H, Rao NA. Immunopathology of necrotising scleritis. *Br J Ophthalmol*. 2008;92:417–419.
8. Young RD, Powell J, Watson PG. Ultrastructural changes in scleral proteoglycans precede destruction of the collagen fibril matrix in necrotizing scleritis. *Histopathology*. 1988;12:75–84.
9. Young RD, Watson PG. Microscopical studies of necrotising scleritis. II. Collagen degradation in the scleral stroma. *BR J Ophthalmol*. 1984;68:781–789.
10. Mohanty V, Subbannayya Y, Najar MA, et al. Proteomics and visual health research: Proteome of the human sclera using high-resolution mass spectrometry. *Omics*. 2019;23:98–110.

11. Zhang P, Karani R, Turner RL, et al. The proteome of normal human retrobulbar optic nerve and sclera. *Proteomics*. 2016;16:2592–2596.
12. Stingl C, Lau SP, van der Burg SH, Aerts JG, van Eijck CHJ, Luider TM. Dataset from a proteomics analysis of tumor antigens shared between an allogenic tumor cell lysate vaccine and pancreatic tumor tissue. *Data Brief*. 2022;44:108490.
13. Y B. Controlling the false discovery rate: A practical and powerful approach to multiple testing. *J Royal Stat Soc*. 1995;57:289–300.
14. Perez-Riverol Y, Bai J, Bandla C, et al. The PRIDE database resources in 2022: A hub for mass spectrometry-based proteomics evidences. *Nucleic Acids Res*. 2022;50:D543–D552.
15. Aghamollaei H, Parvin S, Shahriary A. Review of proteomics approach to eye diseases affecting the anterior segment. *J Proteomics*. 2020;225:103881.
16. Wu Z, Hansmann B, Meyer-Hoffert U, Glaser R, Schroder JM. Molecular identification and expression analysis of filaggrin-2, a member of the S100 fused-type protein family. *PLoS One*. 2009;4:e5227.
17. Mohamad J, Sarig O, Godsel LM, et al. Filaggrin 2 deficiency results in abnormal cell-cell adhesion in the cornified cell layers and causes peeling skin syndrome type A. *J Invest Dermatol*. 2018;138:1736–1743.
18. Furue M. Regulation of filaggrin, loricrin, and involucrin by IL-4, IL-13, IL-17A, IL-22, AHR, and NRF2: Pathogenic implications in atopic dermatitis. *Int J Mol Sci*. 2020;21(15):5382.
19. Akhlaghi M, Karrabi M, Atabti H, Raoofi A, Mousavi Khaneghah A. Investigation of the role of IL18, IL-1beta and NLRP3 inflammasome in reducing expression of FLG-2 protein in Psoriasis vulgaris skin lesions. *Biotech Histochem*. 2022;97:277–283.
20. Choi KH, Lee EB, Yoo CD, et al. Clinical significance of anti-filaggrin antibody recognizing uncitrullinated filaggrin in rheumatoid arthritis. *Exp Mol Med*. 2005;37:546–552.
21. Won P, Kim Y, Jung H, et al. Pathogenic role of circulating citrullinated antigens and anti-cyclic monoclonal citrullinated peptide antibodies in rheumatoid arthritis. *Front Immunol*. 2021;12:692242.
22. Ishikawa K, Sumiyoshi H, Matsuo N, et al. Epiplakin accelerates the lateral organization of keratin filaments during wound healing. *J Dermatol Sci*. 2010;60:95–104.
23. Ahvazi B, Boeshans KM, Rastinejad F. The emerging structural understanding of transglutaminase 3. *J Struct Biol*. 2004;147:200–207.
24. Hoste E, Kemperman P, Devos M, et al. Caspase-14 is required for filaggrin degradation to natural moisturizing factors in the skin. *J Invest Dermatol*. 2011;131:2233–2241.
25. Bhattacharjee M, Balakrishnan L, Renuse S, et al. Synovial fluid proteome in rheumatoid arthritis. *Clin Proteomics*. 2016;13:12.
26. Llop SM, Davoudi S, Stanwyck LK, et al. Association of low Vitamin D levels with noninfectious uveitis and scleritis. *Ocul Immunol Inflamm*. 2019;27:602–609.
27. Ramirez-Miranda A, Nakatsu MN, Zarei-Ghanavati S, Nguyen CV, Deng SX. Keratin 13 is a more specific marker of conjunctival epithelium than keratin 19. *Mol Vis*. 2011;17:1652–1661.
28. Stepp MA, Menko AS. Immune responses to injury and their links to eye disease. *Transl Res*. 2021;236:52–71.
29. Peng X, Nelson ES, Maiers JL, DeMali KA. New insights into vinculin function and regulation. *Int Rev Cell Mol Biol*. 2011;287:191–231.
30. van Heemst J, Jansen DT, Polydorides S, et al. Crossreactivity to vinculin and microbes provides a molecular basis for HLA-based protection against rheumatoid arthritis. *Nat Commun*. 2015;6:6681.
31. Wilson ZS, Witt H, Hazlett L, et al. Context-dependent role of vinculin in neutrophil adhesion, motility and trafficking. *Sci Rep*. 2020;10:2142.
32. Timmermann M, Buck F, Sorg C, Hogger P. Interaction of soluble CD163 with activated T lymphocytes involves its association with non-muscle myosin heavy chain type A. *Immunol Cell Biol*. 2004;82:479–487.
33. Liu Y, Zhang T, Zhang H, et al. Cell softness prevents cytolytic T-cell killing of tumor-repopulating cells. *Cancer Res*. 2021;81:476–488.
34. Nishio Y, Taniguchi H, Takeda A, Hori J. Immunopathological analysis of a mouse model of arthritis-associated scleritis and implications for molecular targeted therapy for severe scleritis. *Int J Mol Sci*. 2021;23(1):341.
35. Elshabrawy HA, Chen Z, Volin MV, Ravella S, Virupannavar S, Shahrara S. The pathogenic role of angiogenesis in rheumatoid arthritis. *Angiogenesis*. 2015;18:433–448.
36. Gonzalez-Teran B, Cortes JR, Manieri E, et al. Eukaryotic elongation factor 2 controls TNF-alpha translation in LPS-induced hepatitis. *J Clin Invest*. 2013;123:164–178.
37. Reck-Peterson SL, Redwine WB, Vale RD, Carter AP. The cytoplasmic dynein transport machinery and its many cargoes. *Nat Rev Mol Cell Biol*. 2018;19:382–398.
38. Tsourouktsoglou TD, Warnatsch A, Ioannou M, Hoving D, Wang Q, Papayannopoulos V. Histones, DNA, and citrullination promote neutrophil extracellular trap inflammation by regulating the localization and activation of TLR4. *Cell Rep*. 2020;31:107602.
39. Seo KY, Lee HK, Kim EK, Lee JH. Expression of tumor necrosis factor alpha and matrix metalloproteinase-9 in surgically induced necrotizing scleritis. *Ophthalmic Res*. 2006;38:66–70.
40. Di Girolamo N, Tedla N, Lloyd A, Wakefield D. Expression of matrix metalloproteinases by human plasma cells and B lymphocytes. *Eur J Immunol*. 1998;28:1773–1784.
41. Di Girolamo N, Lloyd A, McCluskey P, Filipic M, Wakefield D. Increased expression of matrix metalloproteinases in vivo in scleritis tissue and in vitro in cultured human scleral fibroblasts. *Am J Pathol*. 1997;150:653–666.
42. Young TL, Scavello GS, Paluru PC, Choi JD, Rappaport EF, Rada JA. Microarray analysis of gene expression in human donor sclera. *Mol Vis*. 2004;10:163–176.
43. Palexas GN, Puren A, Savage N, Welsh NH. Serum interleukin (IL-1β) in patients with diffuse scleritis. *Scand J Immunol Suppl*. 1992;36:171–172.
44. Sainz-de-la-Maza M, Molins B, Mesquida M, et al. Interleukin-22 serum levels are elevated in active scleritis. *Acta Ophthalmol*. 2016;94:e395–399.

Investigative Ophthalmology & Visual Science